Available online at www.sciencedirect.com
ScienceDirect
Bioorganic & Medicinal Chemistry 15 (2007) 7344–7354
Bioorganic & Medicinal Chemistry

Additional level of information about complex interaction between non-nucleoside inhibitor and HIV-1 reverse transcriptase using biosensor-based thermodynamic analysis

Matthis Geitmann* and U. Helena Danielson

Department of Biochemistry and Organic Chemistry, Uppsala University, Box 576, SE-751 23 Uppsala, Sweden

Received 22 March 2007; revised 27 July 2007; accepted 3 August 2007
Available online 22 August 2007

Abstract—The thermodynamics of the interaction between mutant HIV-1 reverse transcriptase (K103N and Y181C) and a non-nucleoside reverse transcriptase inhibitor (NNRTI), the phenylethylthiazolylurea compound MIV-150, was obtained by determining the temperature dependence of the kinetic rate constants. Large entropic changes in the forward and backward steps of the isomerization between a non-binding competent and a binding competent conformation of the enzyme, as well as in the binding steps, implied the involvement of major structural rearrangements upon interaction with the inhibitor. Despite of the entropic character of the overall interaction, the equilibrium for the binding of inhibitor was found to be predominantly enthalpy-driven. The high affinity and the low affinity interactions of the heterogeneously interacting inhibitor showed different energetics in the analysis, revealing an expectedly higher enthalpic component for the high-affinity interaction. The thermodynamic profiles of the two enzyme variants displayed significant differences, which could not be derived from their kinetics at a single temperature.

1. Introduction

Drug discovery relies on studies of interactions between potential drug compounds and their targets, often enzymes. Initially, studies are limited to interactions with the native target since the aim is simply to identify compounds that interact with the target and interfere with its function. Subsequently, interactions with mutated targets and target homologues are studied as a means of exploring potential resistance and selectivity problems. Moreover, interactions with other proteins and cellular structures, related to pharmacokinetics and ADME-tox properties, may be included in the later stages. The aim is ultimately to select 'the most suitable compound' in a series of analogues representing all conceivable structural variations and an overall drug efficacy perspective. However, in order to rank compounds in terms of 'suitability', it is critical that relevant selection criteria are used. For enzyme–inhibitor interactions selection is generally guided by inhibition data (ideally K_i-values). However, inhibition studies only provide equilibrium based data and with limited possibilities of changing the conditions. Therefore, information about the details of the interaction, such as the kinetics (association and dissociation rate constants) or the effects of altered conditions (chemical composition of the buffer, pH or temperature) on the interaction is rarely obtained. In order to characterize enzyme–inhibitor interactions in detail, we have adopted a surface plasmon resonance (SPR) biosensor in a number of drug discovery projects (see for example Shuman et al.[1]). The present study explores the technique for obtaining thermodynamic data on the interaction between the reverse transcriptase of human immunodeficiency virus type 1 (HIV-1 RT) and non-nucleoside RT inhibitors (NNRTIs).

HIV-RT is an extensively studied target for anti-AIDS pharmaceuticals. At present there are three classes of drugs that target HIV-1 RT: nucleoside-analogue RT inhibitors (NRTIs), nucleotide-analogue RT inhibitors (NtRTIs) and NNRTIs.[2] NRTIs and NtRTIs interact with the active site of HIV-1 RT while NNRTIs comprise a structurally diverse group of allosteric inhibitors. Crystallographic studies have shown that all NNRTIs bind to the same binding site, located in the vicinity of the active site in the p66 subunit of the heterodimeric enzyme.[3–9] Interestingly, the exact position of the entrance

Keywords: Surface plasmon resonance; Thermodynamics; HIV-1 reverse transcriptase; Non-nucleoside inhibitor; MIV-150.
* Corresponding author. Tel.: +46 (0) 18 4714540; fax: +46 (0) 18 558431; e-mail: matthis.geitmann@biorg.uu.se

0968-0896/$ - see front matter © 2007 Elsevier Ltd. All rights reserved.
doi:10.1016/j.bmc.2007.08.018

for the inhibitors remains an object of speculations.[8,10] The binding of NNRTIs to the allosteric site results in short- and long-range conformational changes in the enzyme, and subsequent inhibition of the polymerase activity and impairment of the RNase H activity.[7,11,12]

Although more than 30 structurally different classes of NNRTIs have been described in the past 15 years, only three compounds have been licensed for clinical use so far: nevirapine, delavirdine and efavirenz.[13–17] These are important complements to other types of anti-AIDS drugs since they lack many of the disadvantages of nucleoside and nucleotide-based polymerase inhibitors. Unfortunately, the use of NNRTIs as anti-AIDS drugs is hampered by the rapid development of viral resistance to these inhibitors. A single mutation in the NNRTI-binding pocket can result in high-level resistance. Moreover, NNRTI-resistant HIV variants display cross-resistance to many of the current inhibitors. One strategy for avoiding resistance can be based on designing inhibitors that primarily interact with the polypeptide backbone or with conserved residues in the protein rather than with highly variable residues.[5] A second strategy is to design inhibitors capable of inhibiting multiple variants of HIV-1 RT, for example by designing flexible inhibitors whose interactions with the enzyme are enthalpically favourable.[9] However, the thermodynamics of NNRTI interactions with HIV RT have not been reported in detail previously, so the foundation for such a strategy is lacking.

In two recent studies,[18,19] we have used the surface plasmon resonance (SPR) technique to characterize the interaction between NNRTIs and HIV-1 RT, and the effects of resistance associated mutations on the interaction mechanism. The studies revealed complexities in the interaction mechanism, involving heterogeneity both of the unliganded enzyme and of the enzyme–inhibitor complex. The unliganded enzyme was found to exist in at least two conformations, of which only one is capable of binding the inhibitor. Furthermore, two kinetically distinct enzyme–inhibitor complexes can be formed. Scheme 1 shows the simplest model that adequately describes the kinetics of the interaction.

In the present study we use an SPR-based biosensor to determine the temperature dependence of the kinetic constants and the thermodynamic parameters (ΔG, ΔH and ΔS) in each step of NNRTI and HIV-1 RT interac-

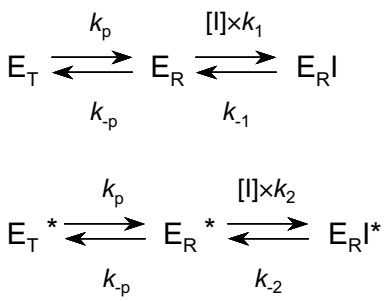

Scheme 1. Interaction model for the binding between HIV-1 RT and NNRTIs.

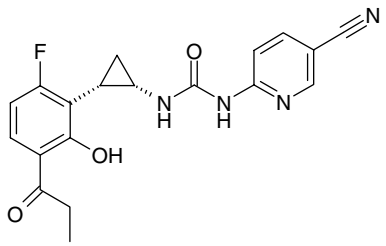

Figure 1. Chemical structure of MIV-150.

tions. Although this technology has previously been shown to be a powerful tool for the thermodynamic characterization of biomolecular interactions,[1,20,21] the extension of deriving thermodynamic parameters from the temperature dependencies of rate constants by this experimental approach has been under debate.[22,23] We would like to emphasize that the herein presented quantities are all apparent under the given assumptions and their significance is discussed. A consequent but reasonably simple nomenclature has been chosen to denote these quasi-thermodynamic parameters[24] ($\Delta G'$, $\Delta H'$ and $\Delta S'$). For this explorative study, we selected a prototype inhibitor, the phenylethylthiazolylurea (urea PETT) compound MIV-150[25] (Fig. 1) and two clinically relevant drug-resistant variants of HIV-1 RT, K103N and Y181C. These substitutions are located in different positions of the NNRTI binding site, and were previously found to interfere with different steps in the inhibitor binding process.[19] The present results are of interest for understanding the NNRTI interaction mechanism and development of effective NNRTIs, and also for understanding general features of molecular interactions.

2. Results

The kinetics of the interaction between HIV-1 RT and the non-nucleoside inhibitor MIV-150 were studied at temperatures ranging from 5 to 35 °C. The experiments and the determination of kinetic constants were based on a previously developed method,[18] which required only slight modifications in order to be applicable over this temperature range. Due to the slow dissociation of the inhibitor at low temperatures, the time between injection cycles had to be prolonged (up to 45 min). Although the pH of the buffer was found to vary 0.32 units from 5 to 35 °C (7.51 and 7.19, respectively) it was not adjusted since we preferred to keep the composition of the buffer constant.

2.1. Temperature dependence of kinetic constants

The effect of temperature changes on the interaction was initially analysed by comparing sets of sensorgrams representing different concentrations of inhibitor obtained at different temperatures (Fig. 2). The temperature clearly influenced both association and dissociation rate constants, apparently to a greater degree for the K103N variant than the Y181C variant. Since the sensorgrams represent all steps in the interaction, that is, both the isomerization of the un-liganded enzyme and the inter-

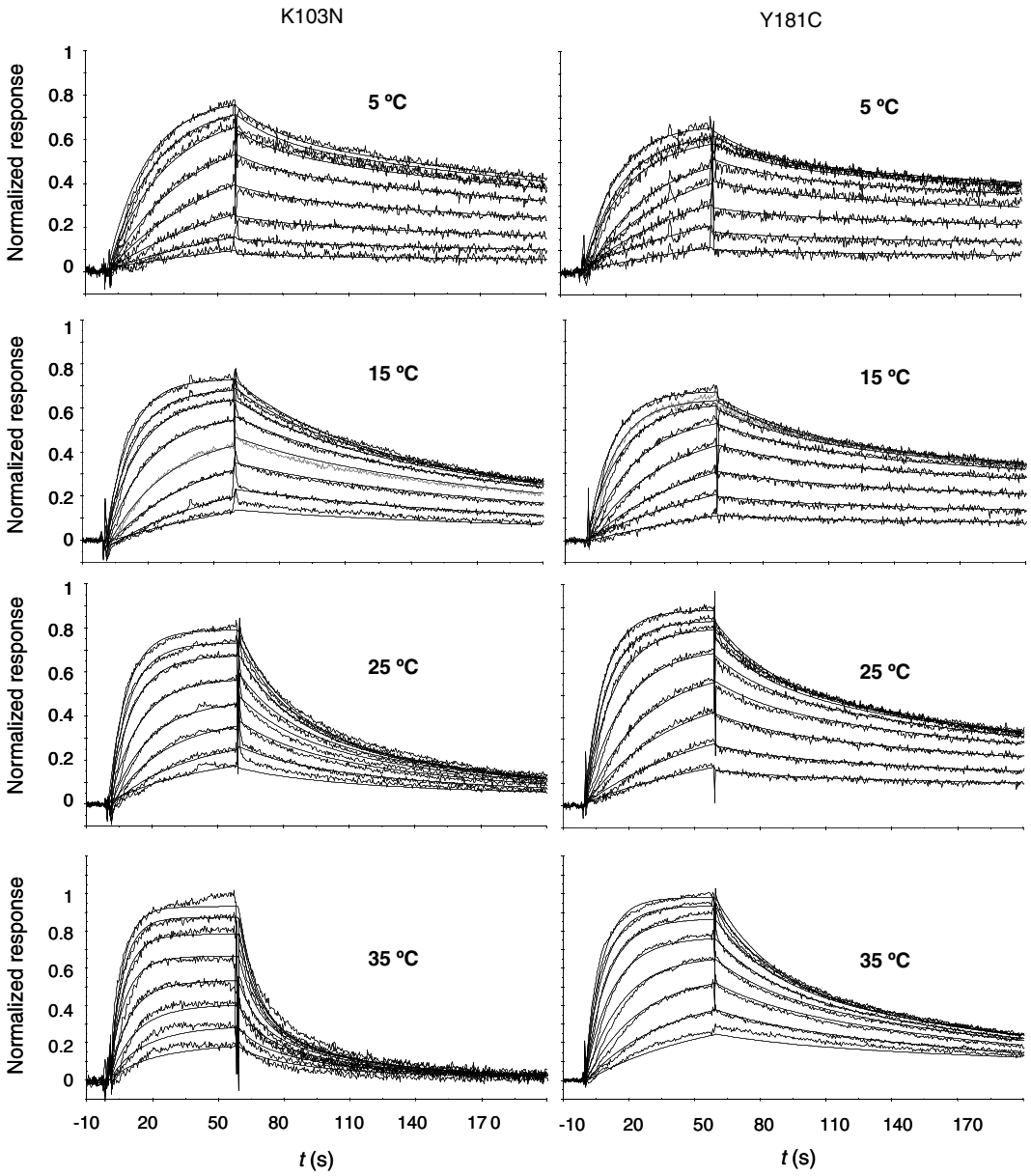

Figure 2. Sensorgrams for the interaction between HIV-1 RT variants (K103N, left column; Y181C, right column) and MIV-150 recorded for inhibitor concentration series (0.04–5.12 μM) at different temperatures (5, 15, 25, 35 °C). The sensorgrams were normalized to 1, assuming a 1:1 binding stoichiometry. Theoretical curves (corresponding to the model in Scheme 1) are overlaid the experimental traces.

action equilibrium, it is not possible to distinguish which steps in the interaction were primarily temperature dependent, or if the temperature had similar effects on all steps. Therefore, in order to quantitatively determine the kinetic rate constants determined for all steps in the system (Scheme 1) at different temperatures, the sets of sensorgrams were subjected to mathematical analysis. The values of the kinetic rate constants and equilibrium constants are presented in Table 1 for the K103N variant and Table 2 for the Y181C variant. Figure 3 shows graphically how the kinetic parameters vary with the temperature.

The kinetic parameters of both the isomerization equilibrium and the interaction equilibrium were temperature dependent. The rate of forming E_R, the binding competent conformation of the enzyme, k_p increased with the temperature, whereas the rate of the opposite step, k_{-p}, decreased with the temperature. This suggests that E_R is favoured under conditions that enhance the flexibility of the protein. A bias of the K103N variant towards a lower K_p than compared to the Y181C variant was observed for all temperatures (P-values 5 °C: 0.816; 15 °C: 0.0132; 25 °C: 0.0001; 35 °C: 0.012).

The temperature dependence of the association and dissociation rate constants was qualitatively the same for both HIV-1 RT variants. Inhibitor association rates varied non-regularly over the measured temperature range, while the rate of inhibitor dissociation increased with increased temperature. As a result, the dissociation constants for the high affinity interaction (K_{D1}) increased at

Table 1. Kinetic constants ± standard deviation for the interaction between HIV-1 RT K103N and the non-nucleoside inhibitor MIV-150

	5 °C	15 °C	25 °C	35 °C
k_1 (s^{-1} M^{-1})	$5.35 \times 10^6 \pm 1.32 \times 10^6$	$6.91 \times 10^6 \pm 5.34 \times 10^6$	$3.57 \times 10^6 \pm 2.71 \times 10^6$	$6.31 \times 10^6 \pm 3.29 \times 10^6$
k_2 (s^{-1} M^{-1})	$1.56 \times 10^6 \pm 8.80 \times 10^5$	$3.45 \times 10^6 \pm 3.33 \times 10^6$	$2.33 \times 10^6 \pm 1.63 \times 10^6$	$2.45 \times 10^6 \pm 1.59 \times 10^6$
k_{-1} (s^{-1})	0.00298 ± 0.00052	0.00477 ± 0.00157	0.0110 ± 0.0035	0.0183 ± 0.0093
k_{-2} (s^{-1})	0.0435 ± 0.0252	0.0321 ± 0.0180	0.0602 ± 0.0202	0.101 ± 0.046
K_{D1} (M)	$5.96 \times 10^{-10} \pm 2.16 \times 10^{-10}$	$9.97 \times 10^{-10} \pm 5.89 \times 10^{-10}$	$4.91 \times 10^{-9} \pm 3.41 \times 10^{-10}$	$3.49 \times 10^{-9} \pm 2.12 \times 10^{-9}$
K_{D2} (M)	$3.57 \times 10^{-8} \pm 2.33 \times 10^{-8}$	$1.43 \times 10^{-8} \pm 1.11 \times 10^{-8}$	$4.48 \times 10^{-8} \pm 4.18 \times 10^{-8}$	$5.18 \times 10^{-8} \pm 2.83 \times 10^{-8}$
k_p (s^{-1})	0.065 ± 0.017	0.097 ± 0.022	0.141 ± 0.031	0.170 ± 0.038
k_{-p} (s^{-1})	4.14 ± 1.28	3.87 ± 2.08	3.20 ± 2.27	2.29 ± 1.14
K_p	65.3 ± 18.14	38.3 ± 11.9	22.4 ± 15.3	13.6 ± 6.5
K_{tot1} (M)[a]	$3.64 \times 10^{-8} \pm 8.66 \times 10^{-9}$	$4.36 \times 10^{-8} \pm 1.52 \times 10^{-8}$	$8.00 \times 10^{-8} \pm 5.08 \times 10^{-8}$	$4.52 \times 10^{-8} \pm 3.86 \times 10^{-8}$
K_{tot2} (M)[a]	$2.41 \times 10^{-6} \pm 2.03 \times 10^{-6}$	$5.65 \times 10^{-7} \pm 3.19 \times 10^{-7}$	$6.00 \times 10^{-7} \pm 2.66 \times 10^{-7}$	$5.74 \times 10^{-7} \pm 1.47 \times 10^{-7}$

The kinetic constants correspond to those defined in Scheme 1: k_p, k_{-p} are the forward and backward rate constants for the isomerization between the two forms of the unliganded enzyme, and k_1, k_{-1} and k_2, k_{-2} respectively are the rate constants for the association and dissociation of the enzyme–inhibitor complex. K_{D1} represents the affinity for high-affinity binding and K_{D2} for low-affinity binding, K_p is the equilibrium constants for the isomerization step, and K_{tot1} and K_{tot2} represent the dissociation constants of the overall equilibrium (both steps).
[a] The values for K_{tot1} and K_{tot2} at 2 °C have been published previously.[19]

Table 2. Kinetic constants ± standard deviation for the interaction between HIV-1 RT Y181C and the non-nucleoside inhibitor MIV-150

	5 °C	15 °C	25 °C	35 °C
k_1 (s^{-1} M^{-1})	$4.80 \times 10^6 \pm 2.04 \times 10^6$	$5.20 \times 10^6 \pm 1.55 \times 10^6$	$4.36 \times 10^6 \pm 1.01 \times 10^6$	$3.91 \times 10^6 \pm 1.27 \times 10^6$
k_2 (s^{-1} M^{-1})	$2.75 \times 10^6 \pm 1.17 \times 10^6$	$5.25 \times 10^6 \pm 2.85 \times 10^6$	$4.58 \times 10^6 \pm 1.78 \times 10^6$	$2.27 \times 10^6 \pm 1.15 \times 10^6$
k_{-1} (s^{-1})	0.00257 ± 0.00088	0.00376 ± 0.00083	0.00623 ± 0.00093	0.00903 ± 0.00532
k_{-2} (s^{-1})	0.0651 ± 0.0389	0.0686 ± 0.0174	0.0773 ± 0.0096	0.0670 ± 0.0381
K_{D1} (M)	$6.27 \times 10^{-10} \pm 3.89 \times 10^{-10}$	$7.90 \times 10^{-10} \pm 2.96 \times 10^{-10}$	$1.50 \times 10^{-9} \pm 4.29 \times 10^{-10}$	$2.89 \times 10^{-9} \pm 2.73 \times 10^{-9}$
K_{D2} (M)	$2.45 \times 10^{-8} \pm 1.42 \times 10^{-8}$	$1.58 \times 10^{-8} \pm 6.55 \times 10^{-9}$	$1.89 \times 10^{-8} \pm 6.05 \times 10^{-9}$	$3.00 \times 10^{-8} \pm 6.92 \times 10^{-9}$
k_p (s^{-1})	0.075 ± 0.017	0.087 ± 0.020	0.101 ± 0.027	0.134 ± 0.016
k_{-p} (s^{-1})	4.80 ± 1.58	4.56 ± 1.17	4.41 ± 1.30	2.98 ± 0.98
K_p	68.0 ± 33.0	54.2 ± 14.8	45.5 ± 13.0	22.3 ± 7.4
K_{tot1} (M)[a]	$2.19 \times 10^{-8} \pm 1.01 \times 10^{-8}$	$4.07 \times 10^{-8} \pm 1.28 \times 10^{-8}$	$6.62 \times 10^{-8} \pm 2.12 \times 10^{-8}$	$6.85 \times 10^{-8} \pm 6.85 \times 10^{-8}$
K_{tot2} (M)[a]	$8.87 \times 10^{-7} \pm 4.11 \times 10^{-7}$	$8.15 \times 10^{-7} \pm 3.64 \times 10^{-7}$	$7.92 \times 10^{-7} \pm 1.18 \times 10^{-7}$	$6.49 \times 10^{-7} \pm 1.92 \times 10^{-7}$

The kinetic constants correspond to those defined in Scheme 1: k_p, k_{-p} are the forward and backward rate constants for the isomerization between the two forms of the unliganded enzyme, and k_1, k_{-1} and k_2, k_{-2} respectively are the rate constants for the association and dissociation of the enzyme–inhibitor complex. K_{D1} represents the affinity for high-affinity binding and K_{D2} for low-affinity binding, K_p is the equilibrium constants for the isomerization step, and K_{tot1} and K_{tot2} represent the dissociation constants of the overall equilibrium (both steps).
[a] The values for K_{tot1} and K_{tot2} at 2 °C have been published previously.[19]

higher temperature. The dissociation constants for the low affinity interactions (K_{D2}) had a minimum at 15 °C.

2.2. Thermodynamic analysis

The thermodynamic parameters of the different steps and the equilibria of the interaction were determined from the temperature dependence of the kinetic constants. The changes in Gibbs energy was calculated directly from the equilibrium constants (Eqs. 1 and 2) while the changes in entropy and enthalpy were calculated by linear regression of equilibrium or rate constants at the four different temperatures (Fig. 4) using Eqs. 3 and 4. The data for 25 °C were compiled in Tables 3–5 and graphically visualized in Figures 5 and 6.

An apparent non-linearity of the plots was observed for most parameters and a non-linear regression analysis including a heat capacity factor[1] provided a better description of most of the data but gave similar parameter estimates. Therefore, for the reason of simplicity, the enthalpy and entropy contributions were assumed independent of the temperature in the present analysis.

2.2.1. Isomerization (pre-equilibrium). The isomerization equilibrium between the two unliganded forms of the enzyme was shifted in favour of the non-binding conformation (E_T), seen as a positive ΔG_{pe} (Fig. 5). ΔH and $T\Delta S$ were positive and larger than ΔG for the K103N variant whereas they were in the same range as ΔG for the Y181C variant. Both the forward and the backward steps were associated with large changes in entropy, but since they cancel out when equilibrium is reached, the net effect is enthalpic. The difference between the two variants was primarily in the relaxation from E_R to E_T, exhibiting larger changes in both enthalpy (P-value 0.0129) and entropy (P-value 0.0066) for K103N than Y181C.

2.2.2. Inhibitor interaction equilibrium. The step where the inhibitor associates with, or dissociates from the enzyme was analyzed for a high affinity and a low affinity interaction (see Scheme 1). The two interactions exhibited different thermodynamic profiles, but the profiles were similar for both enzyme variants, as visualized in Figure 6. The free-energy change at equilibrium upon high-affinity interaction was dominated by a large change in enthalpy, whereas the low-affinity interaction

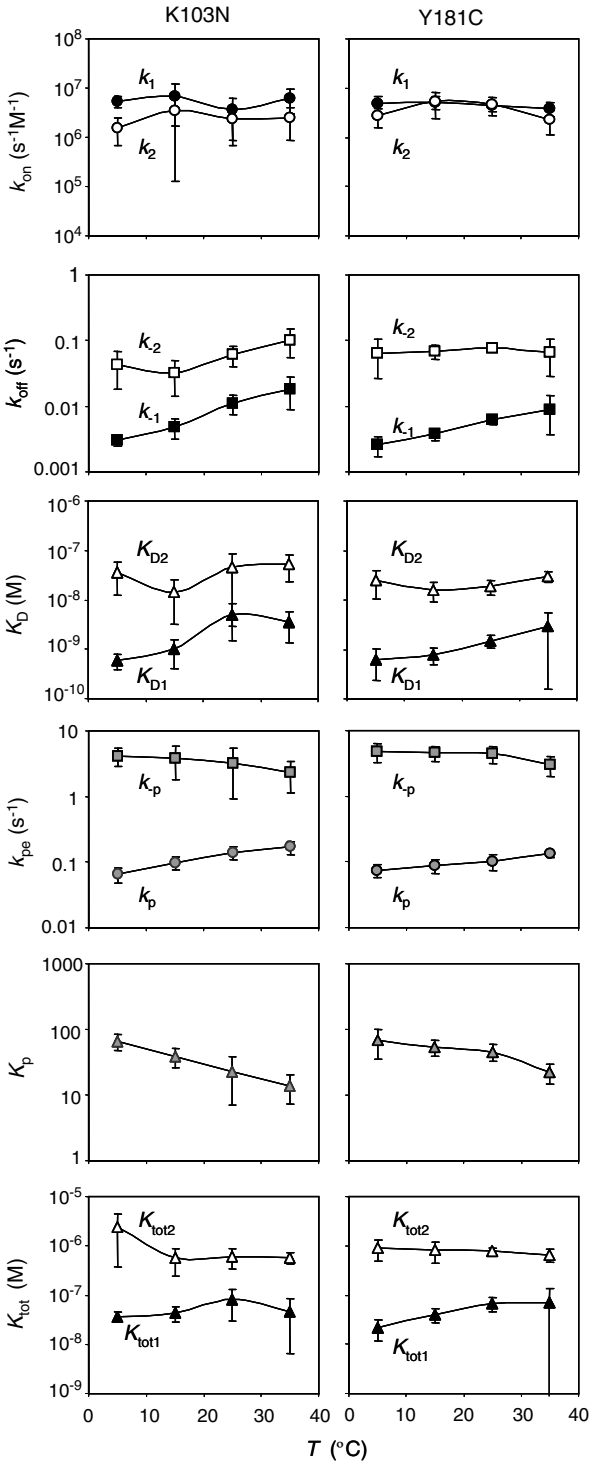

Figure 3. Visualization of kinetic parameters in Tables 1 and 2.

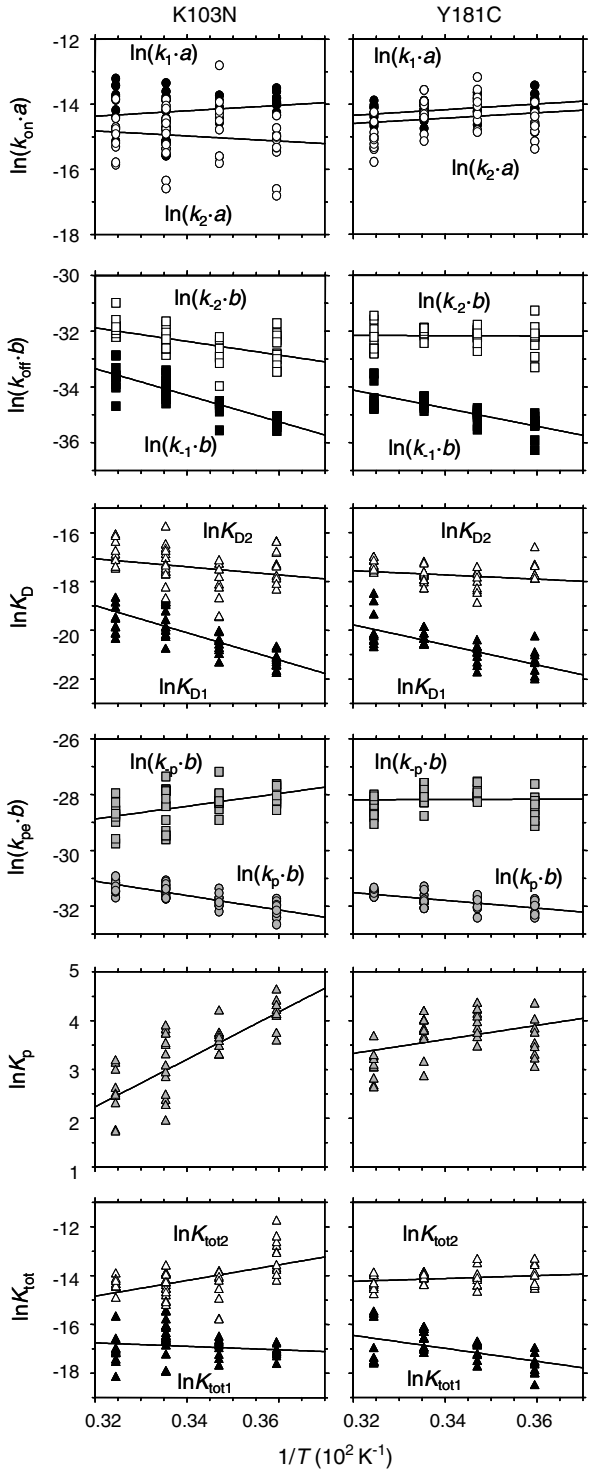

Figure 4. van't Hoff plots (K_p, K_D, K_{tot}) and Eyring plots (k_{on}, k_{off}, k_{pe}) for the interaction between HIV-1 RT variants K103N and Y181C and MIV-150 over a temperature range of 5–35 °C. Determination of thermodynamic and quasi-thermodynamic parameters by linear regression analysis. $a = C \times h/k_b \times T$ and $b = h/k_b \times T$.

was dominated by a large change in entropy. When the thermodynamics was resolved for association and dissociation separately, it was revealed that both steps were associated with large entropic changes and that large enthalpy changes were only involved in the dissociation of the inhibitor.

2.2.3. Overall equilibrium. The overall equilibrium of the interaction between HIV-1 RT and MIV-150 includes both the isomerization and the interaction steps. It was found to be associated with large changes in entropy but a negative change in enthalpy contributes considerably to the high-affinity interaction, especially with the Y181C variant (Fig. 6). For the low affinity interaction

Table 3. Changes in free energy (ΔG), enthalpy (ΔH) and entropy (ΔS) for the pre-equilibrium of MIV-150 interacting with HIV-1 RT K103N and Y181C at 25 °C

	K103N	Y181C
ΔG_{pe} (kJ/mol)	7.22 ± 0.44	9.34 ± 0.22
ΔH_{pe} (kJ/mol)	40.4 ± 5.4	12.0 ± 4.4
ΔS_{pe} (kJ/mol K)	0.111 ± 0.018	0.0107 ± 0.0151
$\Delta G'_{fw}$ (kJ/mol)	77.9 ± 0.1	78.8 ± 0.2
$\Delta H'_{fw}$ (kJ/mol)	21.5 ± 2.4	11.6 ± 2.3
$\Delta S'_{fw}$ (kJ/mol K)	−0.190 ± 0.008	−0.225 ± 0.008
$\Delta G'_{bw}$ (kJ/mol)	70.7 ± 0.5	69.5 ± 0.2
$\Delta H'_{bw}$ (kJ/mol)	−18.9 ± 6.0	−0.354 ± 4.13
$\Delta S'_{bw}$ (kJ/mol K)	−0.300 ± 0.021	−0.235 ± 0.014

The equilibrium thermodynamic parameters ± standard error were determined for 25 °C using Eq. 1a and the equilibrium constants in Tables 1 and 2. Quasi-thermodynamic parameters ($\Delta G'$, $\Delta H'$, $\Delta S'$) for the forward (k_p) and backward reaction (k_{-p}) ± standard error were determined using an Eyring approach and Eqs. 4a and b.

the enthalpy was positive, thus driving the equilibrium towards the unliganded enzyme.

3. Discussion

Previous studies have shown that NNRTI binding to HIV-1 RT can be described by a two-state mechanism, where the un-liganded enzyme is in equilibrium between two different conformations: a binding and a non-binding form which can be assumed to represent the open and the closed form of the NNRTI binding pocket.[18] Since the rate of conversion between the two forms is rate-limiting for the binding of rapidly associating inhibitors, the rates of this isomerization can be obtained from the analysis of interaction data. Furthermore, the interaction of NNRTIs was found to be heterogeneous and a high- and a low-affinity interaction could be identified. The same mechanistic model was found to be valid for the interaction between MIV-150 and the two HIV RT variants studied here, and for the complete temperature range between 5 and 35 °C. The current study provided further details on the interaction that increase our understanding of molecular interactions in general, and of NNRTI–HIV-RT interactions in particular.

3.1. Determination of thermodynamic and quasi-thermodynamic parameters

Eyring's transition state theory originally described the catalysis of substrates into products,[26] but it also applies to the interaction between enzymes and ligands. Whereas the temperature dependency of the equilibrium constants reveals the energetics of the equilibrium, the temperature dependency of the rate constants can be related to quasi-thermodynamic parameters of the individual steps of the interaction, under the assumption that the transmission coefficient $\kappa = 1$ and state of the solvent $C = 1$ M (Eqs. 2a–c). Although the value of κ is expected to be lower than 1 in practice, the few attempts to experimentally determine transmission coefficients have so far resulted in estimates close to unity.[27,28] A simple calculation shows that even when assuming a transmission coefficient of 0.1, the estimated values differ by less than 20% from the values calculated with an assumed transmission coefficient equal to one.

Table 4. Changes in free energy (ΔG), enthalpy (ΔH) and entropy (ΔS) for the high affinity and low affinity interaction between HIV-1 RT and MIV-150 at 25 °C

	K103N		Y181C	
	High affinity	Low affinity	High affinity	Low affinity
ΔG_{int} (kJ/mol)	−48.2 ± 0.4	−43.0 ± 0.4	−50.4 ± 0.2	−44.2 ± 0.2
ΔH_{int} (kJ/mol)	−46.4 ± 6.0	−13.8 ± 6.7	−34.2 ± 5.0	−7.1 ± 4.3
ΔS_{int} (kJ/mol K)	0.009 ± 0.020	0.098 ± 0.026	0.055 ± 0.017	0.123 ± 0.015
$\Delta G'_{on}$ (kJ/mol)	36.1 ± 0.5	37.1 ± 0.5	35.2 ± 0.2	35.2 ± 0.3
$\Delta H'_{on}$ (kJ/mol)	−6.8 ± 5.9	6.4 ± 7.7	−7.2 ± 3.4	−6.7 ± 5.8
$\Delta S'_{on}$ (kJ/mol K)	−0.141 ± 0.020	−0.103 ± 0.026	−0.142 ± 0.012	−0.143 ± 0.020
$\Delta G'_{off}$ (kJ/mol)	84.3 ± 0.2	80.1 ± 0.2	85.6 ± 0.1	79.4 ± 0.1
$\Delta H'_{off}$ (kJ/mol)	39.7 ± 3.4	20.3 ± 4.6	27.0 ± 3.4	0.4 ± 4.0
$\Delta S'_{off}$ (kJ/mol K)	−0.150 ± 0.012	−0.200 ± 0.016	−0.197 ± 0.012	−0.266 ± 0.014

The equilibrium thermodynamic parameters ± standard error were determined for 25 °C using Eq. 1b and the equilibrium constants in Tables 1 and 2. Quasi-thermodynamic parameters ($\Delta G'$, $\Delta H'$, $\Delta S'$) for the association and dissociation ± standard error were determined using an Eyring approach and Eqs. 4a and b.

Table 5. Changes in free energy (ΔG), enthalpy (ΔH) and entropy (ΔS) ± standard error for the overall binding equilibrium between HIV-1 RT and MIV-150 at 25 °C

	K103N		Y181C	
	High affinity	Low affinity	High affinity	Low affinity
ΔG_{tot} (kJ/mol)	−41.0 ± 0.4	−34.9 ± 0.3	−41.1 ± 0.2	−34.9 ± 0.1
ΔH_{tot} (kJ/mol)	−6.09 ± 5.90	26.6 ± 6.5	−22.2 ± 6.1	4.92 ± 3.32
ΔS_{tot} (kJ/mol K)	0.120 ± 0.020	0.209 ± 0.022	0.0659 ± 0.0207	0.134 ± 0.011

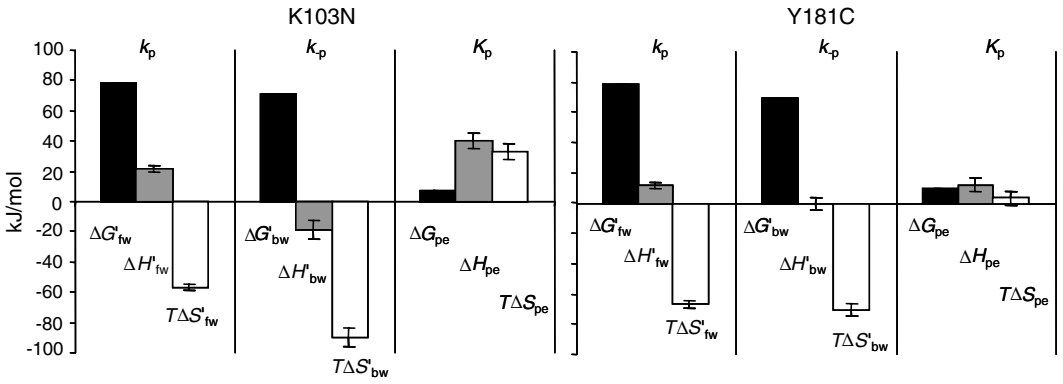

Figure 5. Thermodynamic profiles for the HIV-1 RT K103N and Y181C pre-equilibrium upon interaction with MIV-150 at 25 °C. The changes in enthalpy (ΔH, grey bar), entropy ($T\Delta S$, white bar) and free energy (ΔG, black bar) are shown for the forward and backward steps, as well as for the equilibrium, as indicated by the subscripts.

3.2. The effect of temperature on the isomerization step (pre-equilibrium)

The present investigation of the interaction between NNRTI-resistant HIV-1 RT variants and a urea PETT inhibitor revealed that the pre-equilibrium kinetics of the enzyme was dependent on the temperature. At low temperature the equilibrium was shifted towards the non-binding form of the enzyme, E_T, resulting in higher values for the pre-equilibrium constant K_p (P-values K103N: <0.0001, Y181C: 0.0005). A temperature-dependent equilibrium between different conformational states of the HIV-1 RT has previously been reported concerning the position of the thumb domain.[29] The present study supports the model of a structurally flexible enzyme, which exists in multiple, equilibrating conformations that can be described with statistical distributions.

3.3. The binding-equilibrium for MIV-150 is mainly enthalpy driven

Resolving the free-energy change of the equilibrium between the inhibitor and the enzyme into enthalpy and entropy terms revealed additional information about the nature of the interaction between HIV-1 RT and MIV-150. As for all known NNRTIs, the binding of a urea PETT compound within the NNRTI binding pocket is dominated by hydrophobic interactions. There are also some polar interactions, for example, a single hydrogen bond occurs between the urea nitrogen of the inhibitor and the carbonyl of Lys101.[4,6] Hydrophobic interactions have traditionally been viewed as exclusively entropically driven processes, whereas electrostatic interactions and hydrogen bonding result in changes of enthalpy. It was therefore surprising that for the high-affinity interaction in the interaction equilibrium of MIV-150 and HIV-1 RT, the enthalpy term was larger than the entropy term (P-values K103N: <0.0001; Y181C: 0.0141). By dissecting the thermodynamics of the equilibrium, the enthalpy and entropy contributions to the free energy changes of the association and the dissociation steps could be determined. This analysis revealed that both association and dissociation were governed by entropy terms that were larger than the gain or loss of enthalpy upon binding (P-values association, K103N: 0.0001; Y181C: <0.0001; dissociation, K103N: 0.299; Y181C: <0.0001). However, the entropy parts partially cancelled out and a relatively large negative enthalpy change remains at equilibrium.

An explanation for this can be found in the binding mechanism of NNRTIs to the HIV-1 RT. At the entrance of the binding pocket the inhibitor has to pass a bottleneck in order to enter the binding cavity, requiring a constrained conformation of both enzyme and inhibitor. As an effect of the release from the aqueous solvent, the entropy part of the association of rather hydrophobic NNRTIs was expected to be positive. Since the entropy contribution of a small inhibitor molecule with limited flexibility can be neglected,[30] it can be concluded that the origin of the negative entropy upon association is found in the enzyme. This finding is consistent with the hypothesis that NNRTI binding rigidifies the reportedly flexible structure of the enzyme, concerning mainly the thumb domain.[12,31–33] Hence, it is likely that the entropic solvent effect upon inhibitor binding was compensated by a dynamic effect of the enzyme.

3.4. Thermodynamic analysis reveals complexities in the interaction between HIV-1 RT and MIV-150

The thermodynamic parameters for the high- and the low-affinity interaction were determined separately in the present analysis. The nature of the observed heterogeneity in the inhibitor binding is not yet understood, and might either originate from structural heterogeneity of the enzyme or from the complexity of the underlying binding mechanism.[18] The different energetics for the high- and the low-affinity interaction (Fig. 6) supported the existence of different modes for the inhibitor to interact with the enzyme. Both variants displayed a characteristic difference of 5–6 kJ/mol between high affinity and low affinity binding energies (for both ΔG_{int} and ΔG_{tot}), originating from a difference in the binding enthalpies (ΔH_{int} and ΔH_{tot} for the high and low affinity interaction) of 20–30 kJ/mol. This indicated that the two different complexes are distinguished by the formation

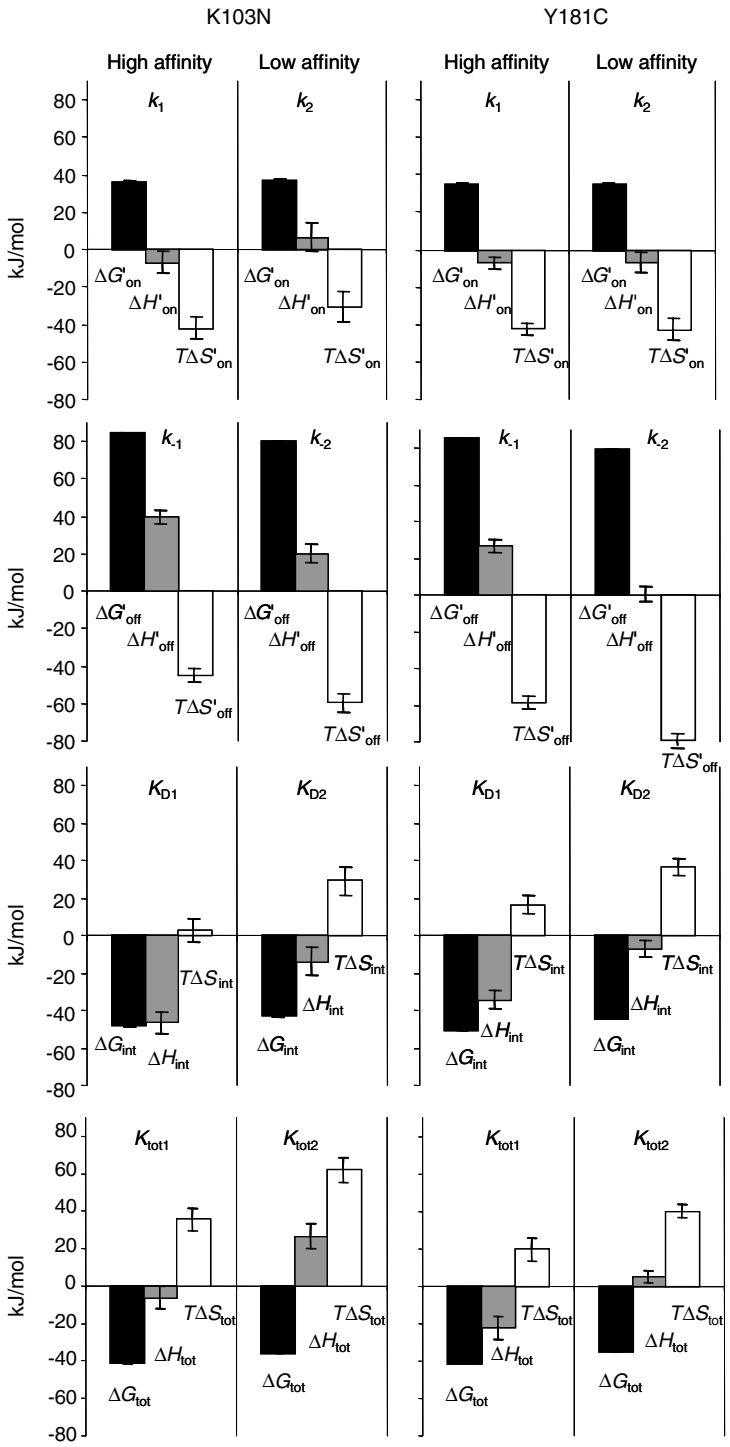

Figure 6. The contribution of changes in enthalpy (ΔH, grey bar), and entropy ($T\Delta S$, white bar) to the change in free energy (ΔG, black bar) for the association, dissociation, interaction equilibrium, and the overall equilibrium with high-affinity binding (left) and low-affinity binding (right) of MIV-150 to HIV-1 RT K103N and Y181C at 25 °C.

of defined electrostatic interactions. Although the differences in the enthalpies exceeded an expected energy contribution of the involved N–H···O hydrogen bond between inhibitor and protein (8 kJ/mol), it is likely that the difference in the free binding energies represents inhibitor binding with and without successful hydrogen bond formation. Furthermore, the high- and the low-affinity interaction revealed different temperature-dependencies, as observed in the different curvatures in the van't Hoff plots (Fig. 4). The change of $\ln K_{D1}$ appeared to be rather linear with the inverse absolute temperature, while $\ln K_{D2}$ showing non-linear tendencies. Applying non-linear regression analysis by introducing a heat capacity factor, the enthalpy appeared to increase with temperatures for the low-affinity interaction (data not shown). It can be speculated that the compensating dynamic effect of the enzyme, which accounts for the negative entropy upon inhibitor association, becomes

less at low temperature, and therefore binding of the inhibitor was governed by an increasing solvent effect of hydrophobic interactions. Interestingly, a similar temperature dependency was reported for the binding of another investigational NNRTI, S-1153, stating that inhibitor binding was enthalpy driven at temperatures above 21 °C and entropy driven at temperatures below 12 °C.[34]

3.5. Differences between the K103N and the Y181C variant

It has previously been suggested that the K103N and the Y181C mutation interfere with different steps in the binding process of an NNRTI.[19] The elucidation of the complex network of forces involved in the interaction revealed further details of the difference between these two resistance variants. The K103N and the Y181C variants showed different energetics for the pre-equilibrium, the binding equilibrium and the overall equilibrium. When only looking at the thermodynamics of the equilibria, the K103N variant displayed a stronger enthalpy contribution than the Y181C variant in the isomerization equilibrium (*P*-value: 0.0001) and the interaction equilibrium (*P*-values high affinity: 0.123; low affinity: 0.448), but vice versa in the overall equilibrium (*P*-values high affinity: 0.061; low affinity: 0.004) (Fig. 6). Furthermore, $\ln K_p$ was rather linearly correlated to $1/T$ in a van't Hoff plot for the K103N variant, whereas clear non-linearity was observed for the Y181C variant (Fig. 4). Obviously, two amino acid substitutions in the binding site cause a large rearrangement of the forces involved in the inhibitor binding process, which remain hidden when only studying the interaction on the kinetic level due to enthalpy–entropy compensation in aqueous systems. Since the inhibition mechanism of these allosteric binders is indirect, it is not surprising that the determined affinity constants do not precisely reflect the fourfold difference in EC_{50} for these resistant variants (wild type, EC_{50} = 5 nM; K103N, EC_{50} = 100 nM; Y181C, EC_{50} = 23 nM; Lotta Vrang, Medivir AB, Huddinge, Sweden, personal communication). It remains therefore to be investigated whether certain thermodynamic parameters would be more suitable to predict the efficacy of non-nucleoside RT inhibitors.

4. Conclusions

The herein presented thermodynamic parameters of complex formation and decay provided additional insights into the nature of the interactions between HIV-1 RT and NNRTIs. Although derived under certain assumptions (C = 1 M, κ = 1) and despite a remaining uncertainty regarding the significance of their absolute quantities, the determined enthalpic and entropic terms of the single reaction steps allowed a rationalization of a contribution of structural features. Their binding mechanism and their thermodynamic profile sets non-nucleoside inhibitors apart from other drugs that target viral enzymes, e.g., HIV protease inhibitors.[1] Even if not all aspects of the complex interaction are well understood yet, the proposed mechanism of inhibitor binding, as well as the previously reported structural effects of NNRTI binding, afforded an interpretation of the experimental data. Further elucidations of the energetics for this class of inhibitors will aid the development of drugs with improved affinities and resistance profiles.

5. Experimental

5.1. Enzymes and inhibitors

The HIV-1 RT (BH10 isolate) variants K103N and Y181C were expressed in *Escherichia coli*, strain BL21 (DE3) and were purified as described by Lindberg et al.[6] The K103N variant has an additional E478Q substitution in order to extinguish the RNase H activity. MIV-150 was synthesized at Medivir, Huddinge, Sweden, and dissolved in dimethyl sulfoxide (DMSO) to give a stock solution of 10 mM.

5.2. Determination of interaction kinetic parameters

Measurements of interactions between HIV-1 RT and MIV-150 were performed at 5, 15, 25 and 35 °C using a Biacore 2000 instrument (Biacore AB, Uppsala, Sweden), essentially as described previously.[18] The enzyme was immobilized by amine coupling to the surface of a CM5 sensor chip (Biacore) and interaction studies were conducted using a running buffer consisting of: 10 mM Hepes, pH 7.4, 150 mM NaCl, 3 mM EDTA and 0.005% surfactant P20 (polyoxyethylenesorbitan), (HBS-EP buffer, Biacore), with addition of 3% (v/v) DMSO. The DMSO stock solution of MIV-150 was diluted in the running buffer and injected for 60 s in automated cycles over the immobilized enzyme in concentration series (0.01–5.12 μM) at a flow rate of 50 μl/min. The flow system was washed with running buffer containing 20% (v/v) DMSO between sample injections. Injections of buffer alone, 'blank injections', were included in each experimental series and the blank responses were subtracted from the inhibitor responses. Experiments were performed at least nine times. Each concentration series was analyzed simultaneously by using non-linear regression analysis (global fitting) with the BIAevaluation program version 3.0.2 (Biacore). The rate constants for the interaction between HIV-1 RT and NNRTIs (k_p, k_{-p}, k_1, k_{-1}, k_2, k_{-2}) were determined using the interaction model presented in Scheme 1. In order to compensate for a baseline drift, or bulk changes between the association and the dissociation phases, additional mathematical expressions were included in the analysis models when needed. Equilibrium constants for the isomerization step $K_p = k_{-p}/k_p$ and the interaction step $K_{Dn} = k_{-n}/k_n$, (where n = 1 for the high-affinity site and 2 for the low affinity site) were calculated from the rate constants. The dissociation constant of the overall equilibrium K_{tot} (both steps) was calculated by $K_{tot1} = K_p \times K_{D1}$ and $K_{tot2} = K_p \times K_{D2}$, respectively.

5.3. Determination of thermodynamic parameters

Thermodynamic parameters were determined essentially as described previously.[1] The overall change in free energy (ΔG_{pe}) for the isomerization step (pre-equilib-

rium) and the interaction steps (ΔG_{int}) was calculated for each temperature directly from the equilibrium constants K_p and K_D, respectively, using

$$\Delta G_{pe} = RT \ln K_p \quad (1a)$$

or

$$\Delta G_{int} = RT \ln K_D \quad (1b)$$

(R is the gas constant and T the absolute temperature).

The $\Delta G'$ for the individual steps in each equilibria were also calculated for each temperature from the corresponding rate constants, using Eqs. 2a–c. These also included the Boltzmann constant (k_b), the Planck constant (h), a term for the state of the solvent (C, here set to 1 M), and the transmission coefficient κ (here set to 1).

The $\Delta G'$ for association ($\Delta G'_{on}$) for each of the two interactions was based on the second order rate constants k_n (k_1 for the high-affinity site and k_2 for the low-affinity site)

$$\Delta G'_{on} = -RT \ln \left(k_n \frac{C \times h}{k_b \times T \times \kappa} \right) \quad (2a)$$

Similarly, $\Delta G'$ for dissociation ($\Delta G'_{off}$) for each of the two interactions was based on the first order rate constants k_m (k_{-1} for the high-affinity site and k_{-2} for the low-affinity site, respectively):

$$\Delta G'_{off} = -RT \ln \left(k_m \frac{h}{k_b \times T \times \kappa} \right) \quad (2b)$$

The corresponding equation was used for calculating the $\Delta G'$ for the forward and backward steps of the isomerization equilibrium ($\Delta G'_{fw}$, and $\Delta G'_{bw}$, respectively):

$$\Delta G'_{fw} \text{ or } \Delta G'_{bw} = -RT \ln \left(k_m \frac{h}{k_b \times T \times \kappa} \right) \quad (2c)$$

using the matching first order rate constants (k_p or k_{-p}).

The enthalpy and entropy changes of the equilibria studied, ΔH and ΔS, respectively, were determined by linear regression analysis from Eqs. 3 (van't Hoff analysis) assuming temperature independence of these parameters.

$$\ln K_p = \frac{\Delta H_{pe}}{RT} - \frac{\Delta S_{pe}}{R} \quad (3a)$$

$$\ln K_D = \frac{\Delta H_{int}}{RT} - \frac{\Delta S_{int}}{R} \quad (3b)$$

Similarly, the quasi-thermodynamic parameters for the individual steps ($\Delta H'_{fw}$, $\Delta S'_{fw}$, $\Delta H'_{bw}$, $\Delta S'_{bw}\Delta H'_{on}$, $\Delta S'_{on}$, $\Delta H'_{off}$ and $\Delta S'_{off}$) were estimated using a transition state theory-based approach according to Eyring:

$$\ln \left(k_n \frac{C \times h}{k_b \times T \times \kappa} \right) = -\frac{\Delta H'_x}{RT} + \frac{\Delta S'_x}{R} \quad (4a)$$

$$\ln \left(k_m \frac{h}{k_b \times T \times \kappa} \right) = -\frac{\Delta H'_x}{RT} + \frac{\Delta S'_x}{R} \quad (4b)$$

The nomenclature (index m and n) and the choice of equation are analogous to that used in Eqs. 2a–c above.

Acknowledgments

The authors thank Prof. Torsten Unge for providing the HIV-1 reverse transcriptase and Medivir AB for providing MIV-150. Cynthia F. Shuman is acknowledged for discussions about the experimental design and Johan Åquist and Olle Mattson for discussions about transition state theory and thermodynamic analysis.

References and notes

1. Shuman, C. F.; Hämäläinen, M. D.; Danielson, U. H. *J. Mol. Recognit.* **2004**, *17*, 106.
2. de Clercq, E. *J. Clin. Virol.* **2004**, *30*, 115.
3. Kohlstaedt, L. A.; Wang, J.; Friedman, J. M.; Rice, P. A.; Steitz, T. A. *Science* **1992**, *256*, 1783.
4. Ren, J.; Diprose, J.; Warren, J.; Esnouf, R. M.; Bird, L. E.; Ikemizu, S.; Slater, M.; Milton, J.; Balzarini, J.; Stuart, D. I.; Stammers, D. K. *J. Biol. Chem.* **2000**, *275*, 5633.
5. Ren, J.; Nichols, C.; Bird, L. E.; Fujiwara, T.; Sugimoto, H.; Stuart, D. I.; Stammers, D. K. *J. Biol. Chem.* **2000**, *275*, 14316.
6. Lindberg, J.; Sigurdsson, S.; Löwgren, S.; Andersson, H. O.; Sahlberg, C.; Noreen, R.; Fridborg, K.; Zhang, H.; Unge, T. *Eur. J. Biochem.* **2002**, *269*, 1670.
7. Esnouf, R.; Ren, J.; Ross, C.; Jones, Y.; Stammers, D.; Stuart, D. *Nat. Struct. Biol.* **1995**, *2*, 303.
8. Esnouf, R. M.; Ren, J.; Hopkins, A. L.; Ross, C. K.; Jones, E. Y.; Stammers, D. K.; Stuart, D. I. *Proc. Natl. Acad. Sci. U.S.A.* **1997**, *94*, 3984.
9. Das, K.; Clark, A. D., Jr.; Lewi, P. J.; Heeres, J.; de Jonge, M. R.; Koymans, L. M.; Vinkers, H. M.; Daeyaert, F.; Ludovici, D. W.; Kukla, M. J.; de Corte, B.; Kavash, R. W.; Ho, C. Y.; Ye, H.; Lichtenstein, M. A.; Andries, K.; Pauwels, R.; de Bethune, M. P.; Boyer, P. L.; Clark, P.; Hughes, S. H.; Janssen, P. A.; Arnold, E. *J. Med. Chem.* **2004**, *47*, 2550.
10. Hsiou, Y.; Ding, J.; Das, K.; Clark, A. D., Jr.; Hughes, S. H.; Arnold, E. *Structure* **1996**, *4*, 853.
11. Shaw-Reid, C. A.; Feuston, B.; Munshi, V.; Getty, K.; Krueger, J.; Hazuda, D. J.; Parniak, M. A.; Miller, M. D.; Lewis, D. *Biochemistry* **2005**, *44*, 1595.
12. Sluis-Cremer, N.; Temiz, N. A.; Bahar, I. *Curr. HIV Res.* **2004**, *2*, 323.
13. de Clercq, E. *Chem. Biodiversity* **2004**, *1*, 44.
14. Pauwels, R. *Curr. Opin. Pharmacol.* **2004**, *4*, 437.
15. Campiani, G.; Ramunno, A.; Maga, G.; Nacci, V.; Fattorusso, C.; Catalanotti, B.; Morelli, E.; Novellino, E. *Curr. Pharm. Des.* **2002**, *8*, 615.
16. Buckheit, R. W. *Expert Opin. Invest. Drugs* **2001**, *10*, 1423.
17. Balzarini, J. *Curr. Top. Med. Chem.* **2004**, *4*, 921.
18. Geitmann, M.; Unge, T.; Danielson, U. H. *J. Med. Chem.* **2006**, *49*, 2367.
19. Geitmann, M.; Unge, T.; Danielson, U. H. *J. Med. Chem.* **2006**, *49*, 2375.
20. Myszka, D. G. *Methods Enzymol.* **2000**, *323*, 325.
21. Roos, H.; Karlsson, R.; Nilshans, H.; Persson, A. *J. Mol. Recognit.* **1998**, *11*, 204.
22. Winzor, D. J.; Jackson, C. M. *Anal. Biochem.* **2005**, *337*, 289.
23. Winzor, D. J.; Jackson, C. M. *J. Mol. Recognit.* **2006**, *19*, 389.

24. Eisenberg, D.; Crothers, D. *Physical Chemistry with Applications to the Life Sciences*; Benjamin/Cummings Publishing Co: Redwood City, CA, 1979, p 242.
25. Högberg, M.; Sahlberg, C.; Engelhardt, P.; Noreen, R.; Kangasmetsa, J.; Johansson, N. G.; Öberg, B.; Vrang, L.; Zhang, H.; Sahlberg, B. L.; Unge, T.; Lövgren, S.; Fridborg, K.; Bäckbro, K. *J. Med. Chem.* **1999**, *42*, 4150.
26. Eyring, H. *J. Chem. Phys.* **1935**, *3*, 107.
27. Nam, K.; Prat-Resina, X.; Garcia-Viloca, M.; Devi-Kesavan, L. S.; Gao, J. *J. Am. Chem. Soc.* **2004**, *126*, 1369.
28. Neria, E.; Karplus, M. *Chem. Phys. Lett.* **1997**, *267*, 23.
29. Kensch, O.; Restle, T.; Wohrl, B. M.; Goody, R. S.; Steinhoff, H. J. *J. Mol. Biol.* **2000**, *301*, 1029.
30. Zhou, Z.; Madura, J. D. *Proteins* **2004**, *57*, 493.
31. Bahar, I.; Erman, B.; Jernigan, R. L.; Atilgan, A. R.; Covell, D. G. *J. Mol. Biol.* **1999**, *285*, 1023.
32. Temiz, N. A.; Bahar, I. *Proteins* **2002**, *49*, 61.
33. Shen, L.; Shen, J.; Luo, X.; Cheng, F.; Xu, Y.; Chen, K.; Arnold, E.; Ding, J.; Jiang, H. *Biophys. J.* **2003**, *84*, 3547.
34. Rajendran, S.; Hang, J. Q.; Yang, Y.; Li, Y.; Tsing, S.; Barnett, J.; Cammack, N.; Ahene, A.; Klumpp, K. *Poster abstract*, 13th International HIV Drug Resistance Workshop, Tenerife Sur-Costa Adeje, Canary Islands, Spain, Jun 8–12, 2004; *Antiviral Therapy* **2004**, *9*, 34; International Medical Press Ltd.: London, UK, 2004.